

Novel Materials and Techniques in Condensed Matter

Proceedings of the Twenty-Ninth Midwest Solid State Conference
held 25-26 September 1981 at Argonne National Laboratory, Argonne,
Illinois, U.S.A.

Editors:

G.W. Crabtree

Solid State Science Division, Argonne National Laboratory, Argonne,
Illinois, U.S.A.

and

P. Vashishta

Solid State Science Division, Argonne National Laboratory, Argonne,
Illinois, U.S.A.



NORTH-HOLLAND
NEW YORK • AMSTERDAM • OXFORD

ARTIFICIAL METALLIC SUPERLATTICES

CHARLES M. FALCO AND IVAN K. SCHULLER

Solid State Science Division, Argonne National Laboratory, Argonne, IL 60439

ABSTRACT

The sputtering technique developed by us to prepare artificial metallic superlattices is described. A calculation of the energy distribution of sputtered particles arriving at the substrate is presented, as are Ion Mill Ion Scattering Spectroscopy and X-ray diffraction data on sputtered artificial superlattices. Several examples of interesting physical phenomena exhibited by these materials are given.

INTRODUCTION

Recently we have prepared a new class of artificially layered materials termed Layered Ultrathin Coherent Structure (LUCS)^{1,2}. As shown schematically in Fig. 1, the degree of order in a layered material can vary from that obtained in multilayered films of amorphous or randomly oriented crystallites, to the high degree of registry in a coherently registered epitaxial layered sample (LUCS). "Prototypes" of the three classes of materials represented in Fig. 1 would be Nb/Ge for a multilayered film, Ni/Cu for a Compositionally Modulated Alloy (CMA) and Nb/Cu for a LUCS. Some of the physical properties of LUCS have been discussed in other papers^{1,3-5}. Here we describe in greater detail our technique for preparing LUCS. Also discussed is a calculation of the energy distribution of the sputtered particles arriving at the substrate. This calculation indicates an important advantage sputtering has over evaporation for the deposited material; especially for refractory metals. One example of an interesting physical property, superconductivity, exhibited by the Nb/Cu LUCS system is described. Also described are the magnetic properties of the CMA Ni/Cu system⁶. For more details on other properties, the reader is referred to the literature¹⁻⁶.

SAMPLE PREPARATION

As shown in Fig. 2, two widely separated and shielded high rate magnetron sputtering guns are placed in a diffusion pumped high vacuum system (base pressure $\sim 8 \times 10^{-8}$ torr). The guns use 13 cm o.d., 5 cm i.d. targets of weight ~ 0.3 -1 kgm. Target current densities during sputtering are in the range 10-100 mA/cm² at voltages of 100-800 V. These parameters give deposition rates of 10-200 Å/sec at the substrate. We find the rates from the guns to be very stable and reproducible run-to-run so that active feedback control is not necessary. The rates are determined by the total power to the guns (IxV) with an Ar gas pressure dependence of the rate at fixed power of less than 0.5%/mTorr in the typical region of operation. Ar pressure is regulated to better than

MULTILAYER
FILM

COMPOSITION
MODULATED
ALLOY (CMA)

LAYERED ULTRATHIN
COHERENT STRUCTURE
(LUCS)

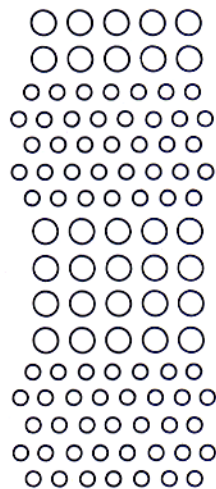
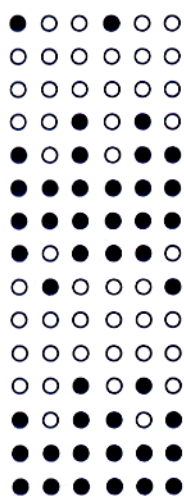
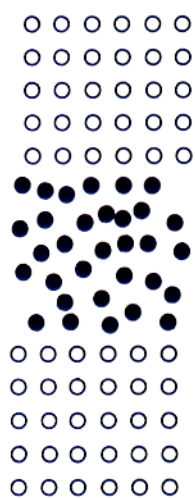


Fig. 1. Schematic representation of degree of order in various classes of layered materials.

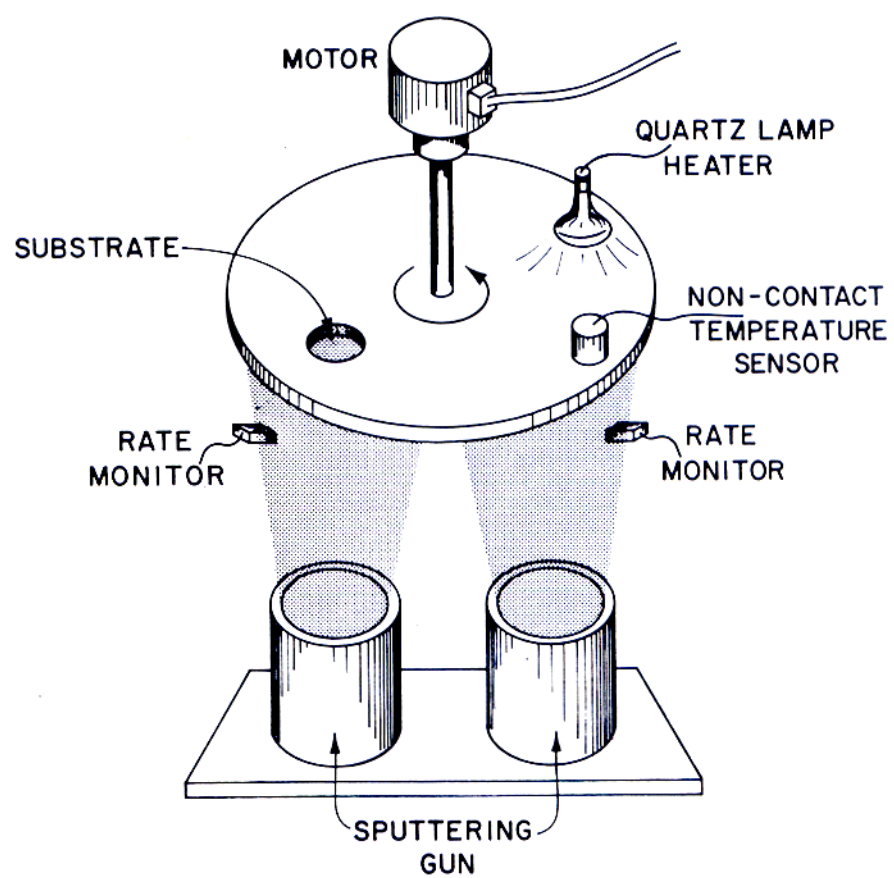


Fig. 2. Sputtering system used for the preparation of artificial metallic superlattices.

0.1mTorr. Pressure is measured both by an ionization gauge and by a capacitance transducer. The rates are monitored during deposition using two quartz crystal oscillators.

The substrates (single crystal 90° or 0° oriented sapphire, mica, MgO, etc.) are held on a rotating platform whose temperature is controlled using a non-contact temperature sensor and quartz lamp heater in a feedback configuration. This allows the substrate temperature to be varied from room temperature to approximately 400 °C to within an accuracy of ± 2 °C. This temperature control is important, as can be seen from Fig. 3 where we show x-ray diffraction data from a series of Ag samples grown on mica at various temperatures (in collaboration with M. Khan). At room temperature the dominant feature is from the (111) texture; but there is a significant fraction of (200) present. The (200) line disappears when grown at higher temperatures and from transmission Laue measurements (not shown here), the Ag is found to grow epitaxially as a (111) oriented single crystal only at the highest temperature of 270 °C. Below this temperature, the Laue measurements show both crystalline spots and polycrystalline rings.

Blackbody radiation from the substrate platform is the dominant heat loss mechanism, and this is what presently limits the upper substrate temperature in our system. The platform can be raised or lowered to change the distance of the substrates from the guns to be in the range from 0.5 to 30 cm. As will be discussed later, this distance can also be an important parameter for obtaining epitaxial growth.

A possible advantage of sputtering over thermal deposition techniques is that control of both the sputtering pressure and of the target/substrate distance allows control of the energy distribution of particles arriving at the substrate. This can easily be seen since typical sputtering pressures are in the range 1-20 mTorr. Conveniently, this corresponds to mean free paths of from a fraction of a centimeter to many centimeters. Thus we can adjust the parameters of our system (pressure and distance) to cause the sputtered particles to arrive either with no energy loss or with a large energy loss due to many collisions with the Ar gas. To see this effect more exactly, we have calculated the energy distribution of sputtered Nb and Cu particles arriving at the substrate for various target to substrate distances⁷. This is shown in Fig. 4 for the case of Nb. Notice that as the above qualitative discussion indicated, the higher the sputtering pressure the closer the final distribution is to the thermal Maxwell-Boltzman distribution of the sputtering gas. A comparison (Fig. 5) of the energy distribution of sputtered and evaporated Nb (for identical rates at the substrate) shows the sputtered distribution to be sharper with a peak energy lower than that of evaporated Nb. This effect is most pronounced for refractory materials.

For the preparation of epitaxial multilayers, it is important for the temperature of the substrate as well as the deposition rates to be high enough to promote epitaxy⁸. At the same time care should be taken that the energy of the particles arriving at the substrate is low enough to avoid disrupting the already formed layers. This is easily accomplished using sputtering since the energy distribution and peak energy can be manipulated by changing sputtering pressures and substrate to target distance.

STRUCTURE

Multilayers of Nb/Cu, Nb/Ti, Nb/Ni, Ni/Ag and Ni/Mo have been prepared using the technique described above. Nb/Cu has been most extensively studied to

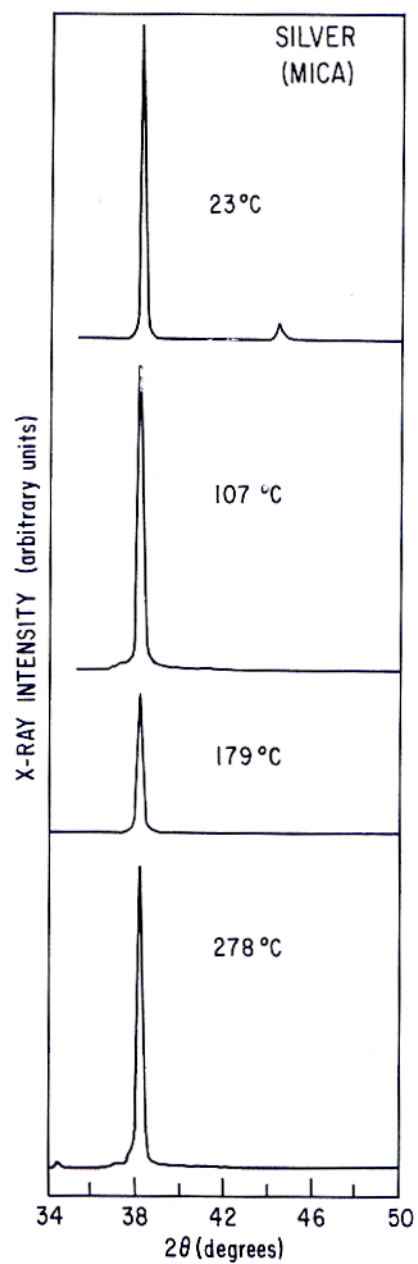


Fig. 3. Bragg x-ray diffraction data from a series of Ag samples grown on cleared mica substrates at four different temperatures.

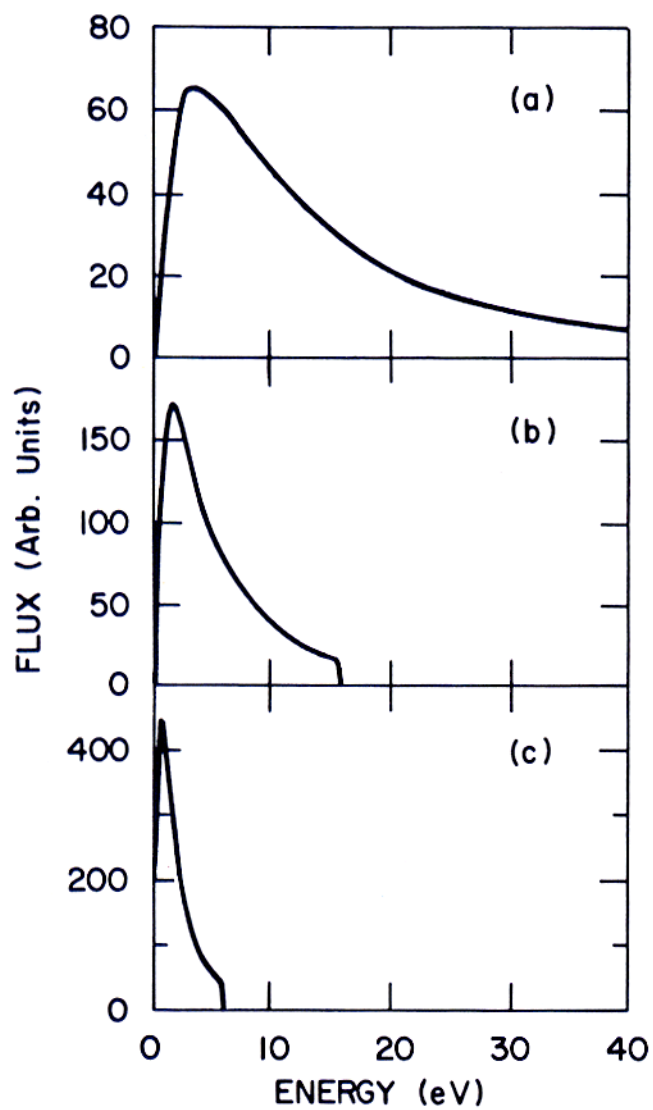


Fig. 4. Calculated Nb energy distribution for various distances traveled from the target with Ar gas pressure 10 mTorr. Distances are a) 0 cm, b) 3 cm, c) 6 cm.

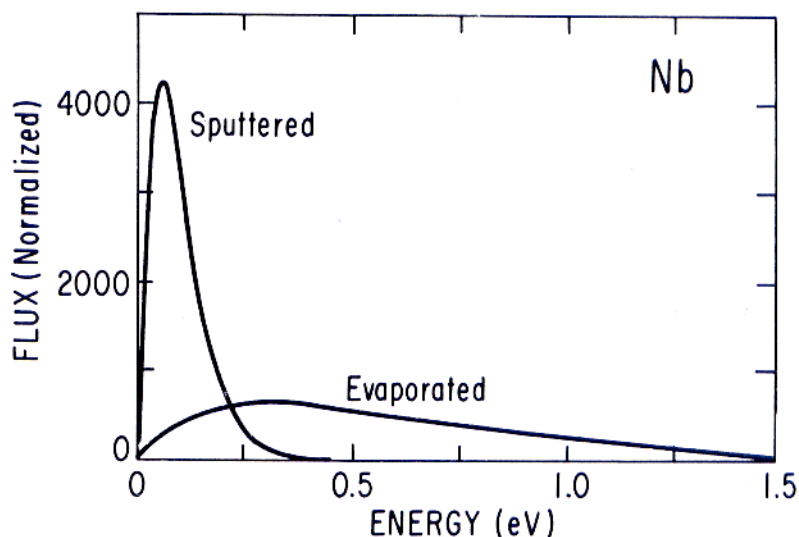


Fig. 5. Comparison of calculated final energy distributions for sputtered and thermally evaporated Nb.

date, so our discussion of structural characteristics will emphasize this material.

Composition determination as a function of depth into the sample with resolution at a scale down to the atomic level is desirable so that the nature of the interface between layers can be studied. There are several surface analysis probes available with depth resolution on roughly the atomic scale; Auger and Ion Scattering Spectroscopy (ISS). The difficulty with ion mill Auger spectroscopy for this purpose is two-fold. The escape depth for the Auger electrons is energy dependent, but even in the most favorable case is ~ 20 Å. Therefore, the Auger signal is only indicative of the chemical composition averaged over at least a 20 Å depth, i.e., approximately 8-10 atomic layers. An additional problem is that the process of ion milling causes significant intermixing of the layers as well as cratering which tends to destroy the layered structure⁹. In order to obviate the finite escape depth problem inherent in the Auger measurements, ion mill ISS measurements have also been performed. Figure 6 shows the ratio of the Cu to Nb composition for a Nb(65 Å)/Cu(65 Å) sample as a function of ion milling time as determined using 1 keV $^{20}\text{Ne}^+$ ions. For the first layer one observes essentially 100% composition modulation; however, intermixing problems caused by the ion milling can clearly be seen to distort the results for subsequent layers. The conclusions from

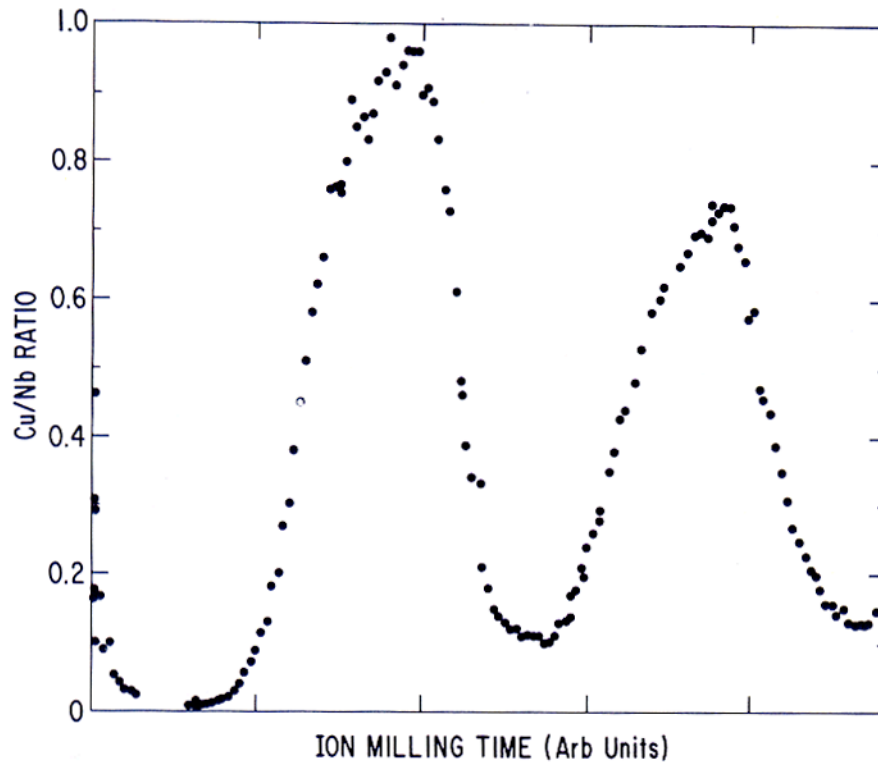


Fig. 6. Dependence of Nb to Cu ratio determined from ISS amplitudes as a function of ion milling time (distance into sample) for a Nb (65 Å)/Cu(65 Å) sample.

these measurements are that the chemical composition of these materials is modulated but that ion milling techniques are not useful for layer thicknesses below ~ 40 Å.

To study the crystal structure we have performed both standard θ - 2θ X-ray scattering and Laue X-ray scattering on a variety of Nb/Cu, Nb/Ti Nb/Ni and Ni/Ag samples. Since for the case of θ - 2θ scans the X-ray momentum transfer is perpendicular to the layers this measurement is only sensitive to structural changes perpendicular to the layers. A one dimensional model calculation assuming 100% composition modulation indicates that characteristic peaks should arise due to scattering by the superlattice planes². The layer thickness ($\lambda/2$) is given by the simple formula

$$\lambda = \frac{\lambda_x}{2} \frac{1}{\sin\theta_i - \sin\theta_{i+1}} \quad (1)$$

where λ_x is the X-ray wavelength and i and $i+1$ refer to adjacent diffraction peaks. Figure 7 shows the measured and calculated X-ray intensities vs 2θ for a series of Nb/Cu samples. We should stress that the existence of a large number of superlattice reflections implies that the position of atomic planes

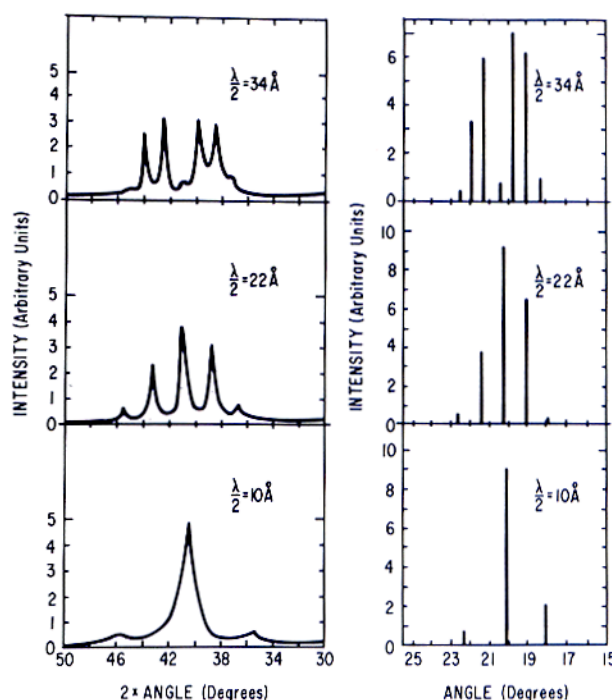


Fig. 7. Measured and calculated X-ray diffraction patterns for a series of Nb/Cu samples of different layer thickness ($\lambda/2$).

perpendicular to the layers is correlated. As in any anisotropic system, several coherence lengths can be defined. In particular, the X-ray measurement

described above gives a lower limit on the coherence of the Nb/Cu superlattice in the z direction (perpendicular to the layers) of ~ 200 Å for superlattice wavelengths in the range 20-70 Å. For superlattices outside this range, the superlattice X-ray peaks merge into a central peak or peaks.

PHYSICAL PROPERTIES

An area of much promise for the observation of effects due to the imposition of a superlattice on a metal is in the phenomenon of superconductivity. In this case the relevant length is the superconductive coherence length (1.6 μm for Al, 380 Å for Nb, etc.), which is long compared to the layer thicknesses which can already be reliably prepared.

We (in collaboration with I. Banerjee and Q. S. Yang) have made both inductive and resistive measurements of the superconductive T_c 's of a series of Nb/Cu samples ranging in layer thickness from 5 Å to 5000 Å³. In all cases the total sample thickness was ~ 1 μm . The T_c 's measured inductively or resistively on these samples are in close agreement, with the narrow resistive transition width (~ 60 mK) indicating the absence of large distribution of inhomogeneities.

The superconducting transition temperatures are a function of layer thickness; for Nb/Cu the transition temperatures start at the 9 K value characteristic of Nb (prepared under identical conditions) and decrease monotonically with decreasing layer thickness (see Fig. 8). Above 200 Å, the changes in T_c

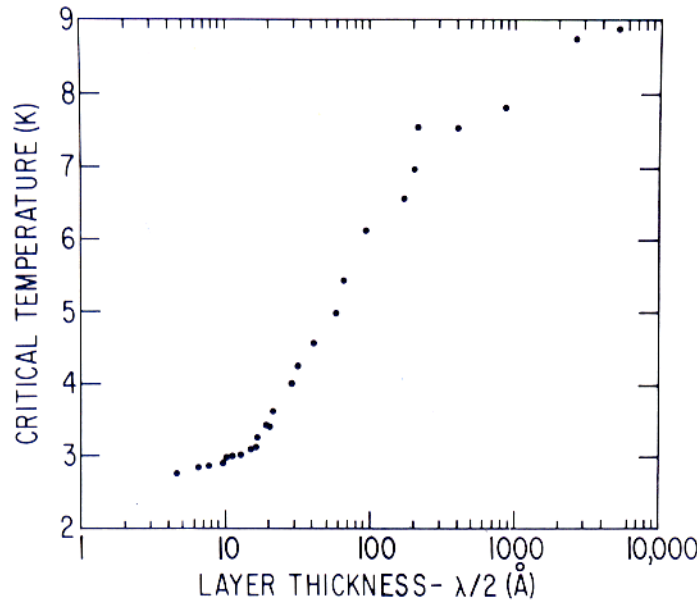


Fig. 8. Measured superconducting transition temperature versus layer thickness ($\lambda/2$) for a series of Nb/Cu samples.

versus layer thickness can be explained, with no adjustable parameters, by proximity effect theories¹⁰. Below 200 Å, this data can also be explained by proximity effect theories; however, it is necessary to invoke a decrease in the transition temperature of Nb as the layer thickness is reduced. Thus for the thin layers (< 200 Å) one obtains T_c of the Nb as a parameter. The decrease in the T_c of Nb inferred from these measurements is in qualitative agreement with measurements of T_c 's for thin single layer Nb films¹¹. Such decreases in T_c for Nb have been earlier ascribed¹² to changes in the density of states at the Fermi surface N_0 .

Magnetism is another phenomenon where superlattice effects might be observed. We are presently studying the growth of several possible magnetic LUCS superlattices. To date, we have obtained measurements (in collaboration with J. B. Ketterson and J. Q. Zheng) on partially layered Cu/Ni samples⁶. Here, the materials are mutually soluble so that the composition can be modulated around some average value but complete layering is not obtained. This corresponds to the Composition Modulated Alloy (CMA) case shown in Fig. 1. Cu/Ni samples were prepared on mica substrates using a dual electron beam gun evaporator rather than by sputtering. Structural studies demonstrate that these Cu/Ni samples are preferentially oriented along the (111) direction. Laue diffraction studies also show that the material is crystalline in the x-y plane.

We have measured the magnetization of Cu/Ni over a wide magnetic field (0-10 kG) and temperature (5-350 °K) range. These results are shown in Fig. 9 and 10. The data show magnetizations reduced from that of pure Ni in agreement with neutron scattering experiments¹³ and band structure calculations¹⁴. The saturation magnetization varies with composition amplitude and is independent of modulation wavelength. The Curie temperature is amplitude independent and decreases with decreasing wavelength. The magnetic field dependence of the magnetization implies that there is only a small magnetostrictive term, indicating the absence of large strains in this material. The temperature dependence of the saturation magnetization indicates a Curie point independent of modulation amplitude. All of the observed properties are consistent with the idea that the properties of Cu/Ni samples are determined by thin film effects rather than by anything due to a superlattice. Clearly, more ideal magnetic materials are required, and we are working on this problem.

SUMMARY

Compositional (Ion Mill Auger and Ion Scattering Spectroscopy) and X-ray structural studies show that metallic superlattices can be prepared by sputtering. Calculations indicate that this in part may be due to the role that the sputtering gas plays in determining the energy distribution of atoms arriving at the substrate. Nb/Cu samples have been prepared which show large range structural coherence (~ 200 Å) perpendicular to the layers. Superconducting T_c 's and anisotropic H_c 's have been obtained which are indicative of the layered nature of these materials. To date, work on magnetic metals has been limited to Compositionally Modulated Alloys (CMA's). Work is underway to fabricate LUCS quality superlattices using magnetic materials.

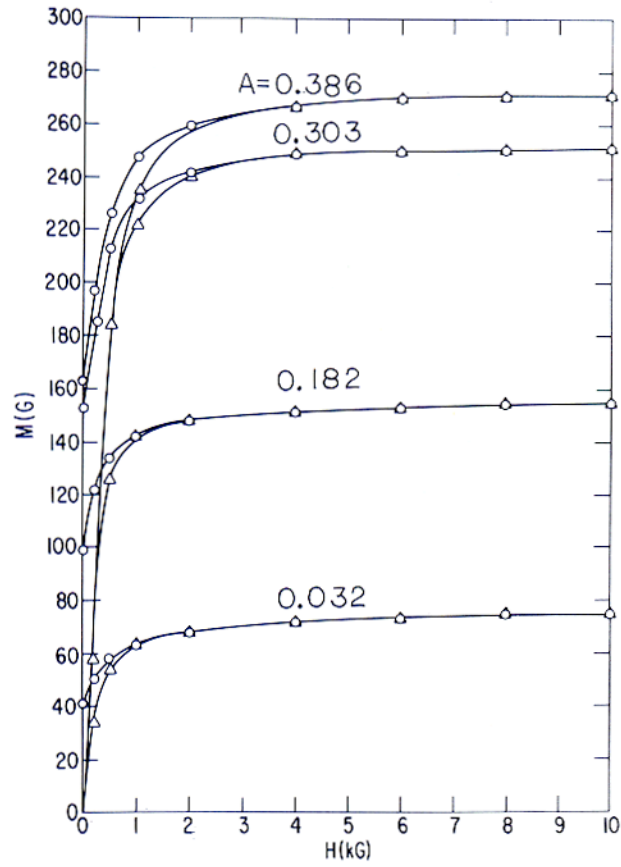


Fig. 9. Magnetization versus H for a 60% Cu/40% Ni sample with $\lambda/2 = 15.2 \text{ \AA}$. Four different composition modulation amplitudes obtained from successive annealing are shown. Δ increasing H , \circ decreasing H .

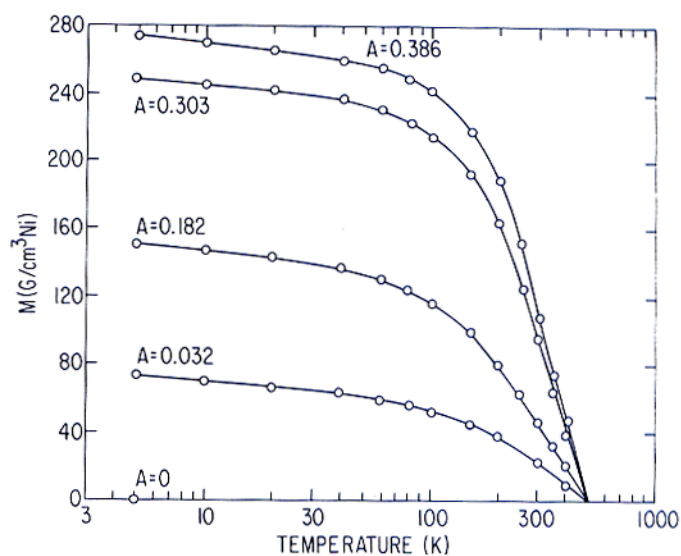


Fig. 10. Temperature dependence of the saturation magnetization for the sample shown in Fig. 8.

ACKNOWLEDGEMENTS

We would like to thank our collaborators: I. Banerjee, R. T. Kampwirth, J. B. Ketterson, M. Khan, K. Meyer, T. R. Werner, Q. S. Yang and J. Q. Zheng on various aspects of this work. We would also like to thank Dr. Gene R. Sparrow for obtaining the ISS spectra on our samples and The Physical Electronics Laboratories who performed some of the Auger measurements. This work is supported by the Office of Naval Research Contract N00014-80-F-0074 and by the U.S. Department of Energy.

REFERENCES

1. I. K. Schuller and C. M. Falco, in Inhomogeneous Superconductors-1979 ed. by D. U. Gubser, T. L. Francavilla, J. R. Leibowitz and S. A. Wolf (American Institute of Physics, New York, 1980), p. 197.
2. I. K. Schuller, Phys. Rev. Letters 44, 1597 (1980).
3. I. Banerjee, Q. S. Yang, C. M. Falco and I. K. Schuller (to be published).
4. I. K. Schuller and C. M. Falco, Surface Science (in press).
5. T. R. Werner, I. Banerjee, C. M. Falco and I. K. Schuller (to be published).
6. J. Q. Zheng, C. M. Falco, J. B. Ketterson and I. K. Schuller, Appl. Phys. Letters 38 424 (1981) and J. Appl. Phys. (in press).
7. K. Meyer, I. K. Schuller and C. M. Falco, J. Appl. Phys. 52 5803 (1981).
8. See, for example, various chapters in Epitaxial Growth, edited by J. W. Matthews (Academic Press, New York, 1975).
9. I. K. Schuller and C. M. Falco, Thin Solid Films (in press).
10. P. G. de Gennes and E. Guyon, Phys. Lett. 3, 168 (1963) and N. R. Werthamer, Phys. Rev. 132, 2440 (1963).
11. S. A. Wolf, J. J. Kennedy and M. Nisenoff, J. Vac. Sci. Tech. 13, 145 (1976).
12. C. M. Varma and R. C. Dynes, in Superconductivity in d and f Band Metals -- Second Rochester Conference edited by D. H. Douglas (Plenum Press, New York, 1976), p. 507.
13. G. P. Felcher, T. Cable, J. B. Ketterson, J. Q. Zheng and J. E. Hilliard Journal of Magnetism and Magnetic Materials, 21, 198 (1980).
14. T. Jarlborg and A. J. Freeman, Phys. Rev. Letters 45, 653 (1980).